

Shorted Circular Microstrip Antennas for $50\ \Omega$ Microstrip Line Feed with Very Low Cross Polarization

Shivraj M. Rathod^{1, *}, Raval N. Awale¹, and Kamla P. Ray²

Abstract—A circular microstrip antenna (CMSA) cannot be fed directly with $50\ \Omega$ microstrip (MS) line, without an inset or an impedance transformer, as all around the periphery the impedance is equally high. The feeding technique such as inset fed or quarter wave transformer makes the antenna geometry asymmetrical. In this paper, a technique using single shorting post and a pair of shorting posts is proposed to match the peripheral impedance of the CMSA with that of the $50\ \Omega$ -MS-line feed for operation around 2.45 GHz. The shorting posts perturb the current distribution on the patch, altering the input impedance at the periphery. By selecting proper shorting posts positions a wide range of impedance has been adjusted without altering the patch geometry. Due to symmetric arrangement of the double shorting posts, the proposed antenna configuration has a very low cross-polarization ratio of better than $-65\ \text{dB}$ at the broadside direction for 2.45 GHz. The simulated results of the directly fed $50\ \Omega$ -MS-line CMSAs are experimentally validated with good agreement.

1. INTRODUCTION

In modern days, the concepts of creating compact and impedance-agile microstrip antennas (MSAs) has attracted increasing attention due to miniaturization and ease of integration with microwave circuits and devices [1–8, 10–12, 14–16]. Compact MSAs have been realized by the simple method of loading the patch by either shorting post (pin) or shorting plate [1–8]. Shorting post is connected between the patch and ground plane, which helps to perturb the surface current distribution on the patch. It also forces the electric field to become zero at that point, thereby modifies various modes of the patch [2, 4]. Shorting posts along the zero field line of fundamental mode of the patch converts half wave length resonator into quarter wavelength, which help to realize compact MSA. Compact and shorted configurations of rectangular, circular and triangular antennas with the shorting post technique have been reported in [2, 4]. Besides realizing compactness, the shorting technique has also been used to obtain dual-frequency response [5], tunability [9], impedance matching [10–12, 14–16], etc. Recently, various configurations of compact and broadband MSAs have been reported using shorting techniques [6–8]. Direct integration of MSA elements with coplanar $50\ \Omega$ microstrip (MS)-line feed on the same plane is highly demanded in on-chip platform, to make a compact electronic system.

A rectangular MSA (RMSA) provides flexibility for directly feeding through $50\ \Omega$ -MS-line along the non-radiating edges [2, 3, 11, 16]. However, there is no flexibility to feed Circular MSA (CMSA) directly with $50\ \Omega$ -MS-line as there are no non-radiating edges all along the periphery [2, 3, 11]. The peripheral input impedance of a CMSA typically varies between 400 and $500\ \Omega$, and necessitates the use of either inset or impedance transformer for MS-line feed. Both these feeding methods make an antenna configuration asymmetrical along the E -plane, which increases the cross-polarization level in the H -plane. Additionally, inset feed becomes unrealizable for some cases at the higher range of microwave

Received 9 January 2018, Accepted 12 March 2018, Scheduled 26 March 2018

* Corresponding author: Shivraj Mahadusing Rathod (rathod.shivraj@gmail.com).

¹ Department of Electrical Engineering, Veermata Jijabai Technological Institute (VJTI), Mumbai, Maharashtra State 400019, India.

² Department of Electronics Engineering, Defence Institute of Advanced Technology (DIAT), Pune, Maharashtra State 411025, India.

frequency. Shorted RMSA configurations directly fed with $110\ \Omega$ -MS-line have been reported [14, 15], which is not a standard characteristic impedance. In addition, it requires additional TRL calibration kit to de-embed the input impedance. It is mostly preferred, at least in lower microwave frequency range, to feed MSA with $50\ \Omega$ -MS-line [16]. In [14, 15], the co-polarization to cross-polarization ratios (CTCR) in H -plane of the pair of shorting posts RMSA have been reported to be lower by 10 dB in comparison with that of a single shorting post RMSA. A CMSA is a preferred radiator, besides being a perfectly symmetric geometry as compared to RMSA. Furthermore, it suppresses the harmonics generated by transmitters/oscillators, which are in multiple of fundamental mode frequency [2, 3].

In this paper, a shorted CMSA with $50\ \Omega$ -MS-line feed using single shorting post and a pair of shorting posts has been presented. A CMSA with a pair of shorting posts gives more than 24 dB suppression of cross-polarization level with respect to a single shorted CMSA in H -plane. This suppression is 14 dB higher than the result presented for a pair of shorting posts RMSA [15]. Proposed shorted CMSAs are fabricated, and measurements have been carried out to validate simulation results. The experimental results are in good agreement with simulated ones. These proposed configurations are designed for 2.45 GHz communication and ISM bands.

2. ANTENNA GEOMETRY

Geometries of proposed shorted CMSA configurations are depicted in Fig. 1. Initially, a conventional coaxial fed CMSA with diameter D has been designed at the fundamental mode frequency equal to 1.8 GHz (widely used operating frequency in various communication systems) with dielectric substrate Arlon. This substrate material has a relative permittivity $\epsilon_r = 2.5$, dielectric thickness $h = 1.59\ \text{mm}$ and loss tangent $\tan \delta = 0.003$. The accurate formula for resonant frequency of a CMSA is

$$f_{nm} = \frac{ck_{nm}}{2\pi a_e \sqrt{\epsilon_e}} \quad (1)$$

where k_{nm} is the m^{th} zero of the derivative of Bessel functions of order n [2, 3]. The value of k_{nm} for the fundamental mode $\text{TM}_{11} = 1.84118$. Parameters c , a_e , and ϵ_e are the speed of light, effective radius and effective dielectric constant of a CMSA, respectively. The radius of the circle $a = 30.01\ \text{mm}$ is calculated using Equation (1). In order to match the impedance of a CMSA at the periphery with $50\ \Omega$ -MS-line feed, a technique of single shorting post and a pair of shorting posts is used. The radius of the shorting post is r , which is introduced at a distance d from the peripheral feed point. The dimensions of the $50\ \Omega$ -MS-line feed are width (W_s) = 4.538 mm and length = 10 mm. Use of MS-line slightly reduces the fundamental mode resonant frequency to 1.74 GHz, because of marginal increase in overall effective dimension of the patch. The analysis of the proposed shorting post loaded CMSA configurations, as shown in Figs. 1(a) and (b), has been carried out using Method of Moment based software IE3D.

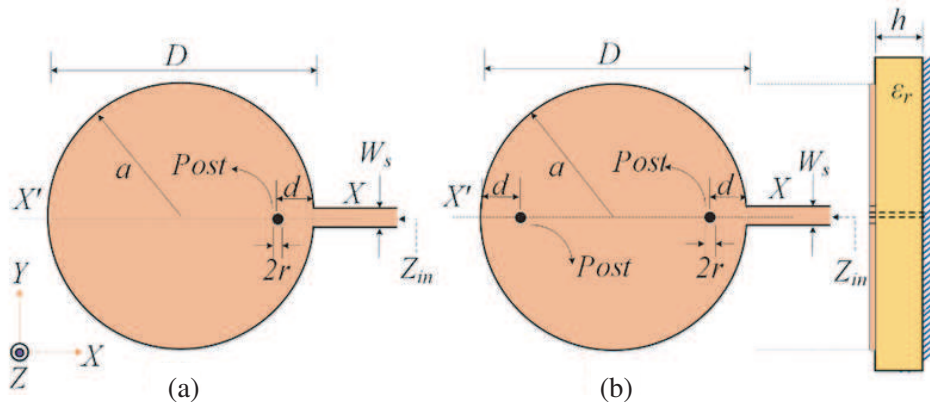


Figure 1. The geometry of shorted CMSA with $50\ \Omega$ -MS-line feed, (a) single shorting post, (b) pair of shorting post with a cross-sectional view.

3. SINGLE SHORTING POST 50 Ω-MS-LINE FED CMSA

A shorting post on a patch modifies the field distribution leading to the change of a resonant frequency of different modes and their input impedance at the periphery. Initially, a single shorting post of radius $r = 0.5 \text{ mm}$ is introduced along the center line XX' at position d from the peripheral feed point as shown in Fig. 1(a). The shorting post modifies the surface current distribution of the fundamental mode (TM_{11}) of the CMSA, which in turn slightly increases its resonant frequency F_F . In addition, a lower resonant mode F_L is also introduced, whose resonant frequency is a function of a position of the shorting posts [2, 4]. For the fundamental TM_{11} mode of the CMSA, the radius of the patch is effectively a distance between zero potential point (center) and the open circuit (periphery). Using the same analogy, the resonant frequency F_L of the peripheral shorted CMSA is calculated. Hence, the effective radius is considered as $a_{e1} = \pi a_e$. With substitution of this value of radius in Equation (1), F_L is reduced to;

$$F_L = \frac{8.791}{a_{e1}\sqrt{\epsilon_e}} \quad (2)$$

where F_L and a_{e1} are defined in GHz and cm, respectively. When the shorting post along the center line moves from periphery to the center, the effective a_{e1} decreases leading to increase in F_L . Hence, for the requirement of compact CMSA configuration with 50 Ω-MS-line-fed, it can be operated at lower order mode frequency F_L . Recently, an analytical approach for calculating the values of F_L with arbitrary location of shorting post has been reported in [13], which is based on the cavity model.

In this paper, investigations have been carried out only for the modified fundamental mode with frequency F_F for the peripheral fed shorting post loaded CMSA. Fig. 2 depicts the surface current distributions for three different positions of a single shorting post CMSA at corresponding frequencies F_F . For a center shorting post, the current distribution is symmetrical on a patch, which is similar to TM_{11} mode. When the shoring post is shifted towards periphery, a current distribution becomes increasingly asymmetrical, and the TM_{11} mode gets modified. This asymmetrical current distribution in the E -plane (Feed axis) results in increase in cross-polar level in the H -plane. Fig. 3(a) depicts the simulated input resistance (R_{in}) and reactance (X_{in}) of a single shorting post loaded CMSA with different shorting positions (d/D ratio). It is observed that as d/D ratio decreases (pin moves from the center to the periphery), i.e., $d/D = 0.5$ to 0.05, the input resistance at the periphery for the corresponding resonance frequency F_F is reduced from 50 to 49 Ω. For the same variation of d/D , the resonant frequency F_F increases from 1.740 to 2.095 GHz, because of the modification in the surface current distribution. Hence, by choosing a proper position of a shorting post, a wide range of input impedance of MS-line-fed CMSA can be adjusted for various ranges of frequency without using other impedance matching techniques. For 50 Ω-MS-line-fed CMSA, when shorting post is kept at $d/D = 0.05$, the input impedance matching is obtained at the frequency $F_F = 2.095 \text{ GHz}$. Fig. 3(b) depicts the

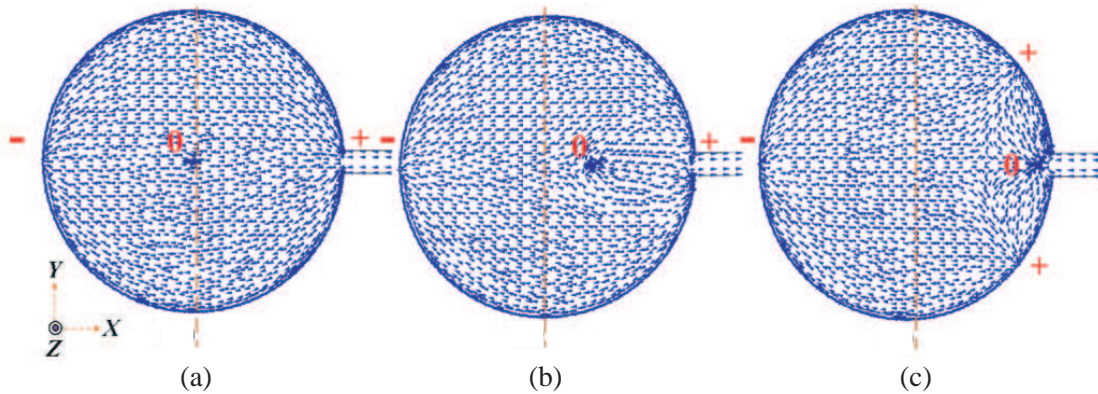


Figure 2. Surface current distribution on single shorting post CMSA with different shorting positions. (a) $d/D = 0.5$ (equivalent to a conventional CMSA), (b) $d/D = 0.3$, and (c) $d/D = 0.05$ at corresponding F_F .

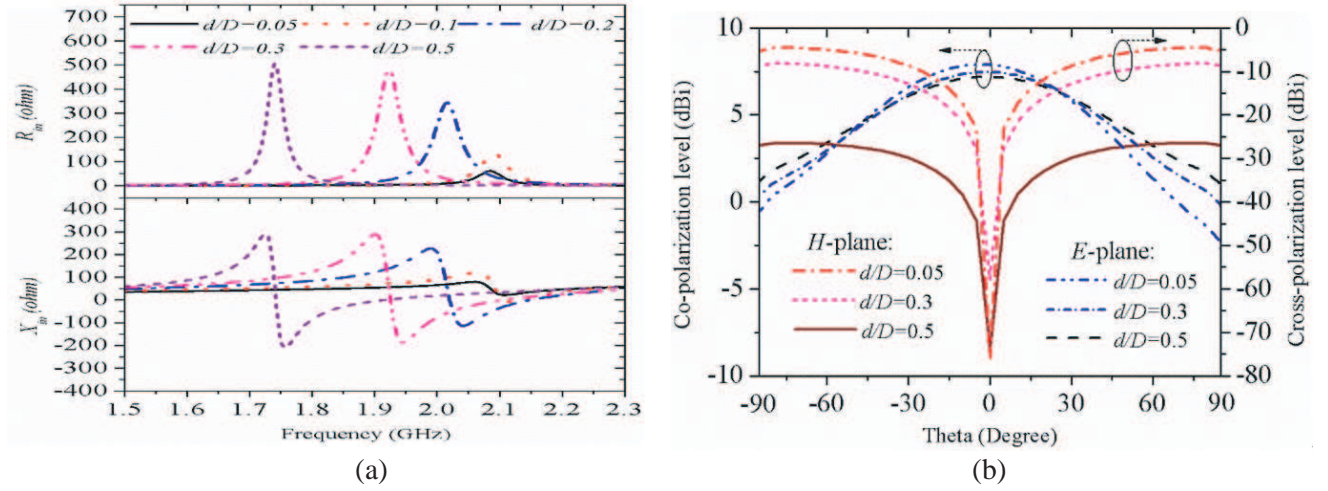


Figure 3. (a) Simulated input resistance and input reactance, and (b) simulated co-polarization in E -plane and cross-polarization in H -plane of a single shorting post loaded CMSA with different d/D ratio. (At $d/D = 0.5, 0.3$ and 0.05 the corresponding modified frequencies are $F_F = 1.74, 1.958$ and 2.095 GHz, respectively).

comparison of simulated co-polarization levels in E -plane and corresponding cross-polarization levels in H -plane of a single shorting post loaded CMSA with different d/D ratios at corresponding modified frequency F_F . The single shorting post loaded in CMSA creates asymmetrical current distribution in the E -plane (i.e., Feed axis), which leads to increase in the cross-polar level in H -plane. It is noticed from Fig. 3(b) that as a shorting post moves from center to the periphery of CMSA, the cross-polarization level in the off broadside direction in the H -plane gets increased from -26 to -5 dBi, while the co-polarization levels in the E -plane remain almost the same.

4. PAIR OF SHORTING POSTS $50\ \Omega$ -MS-LINE FED CMS

To overcome the problem of increased cross-polarization level in H -plane of an asymmetrical single shorting post CMSA, a pair of shorting posts is used, which are symmetrically placed along XX' line of the CMSA as shown in Fig. 1(b). The dimension of the CMSA and substrate parameters are kept the same as that of the single shorting post loaded CMSA. Fig. 4 depicts the surface current distribution

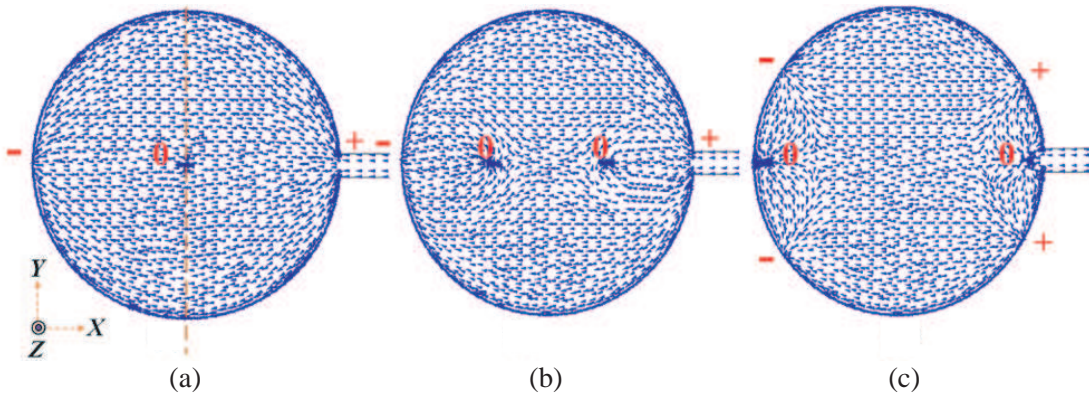


Figure 4. Surface current distribution on the pair of shorting posts CMSA with different shorting positions. (a) $d/D = 0.5$ (equivalent to a conventional CMSA), (b) $d/D = 0.3$, and (c) $d/D = 0.05$ at corresponding F_F .

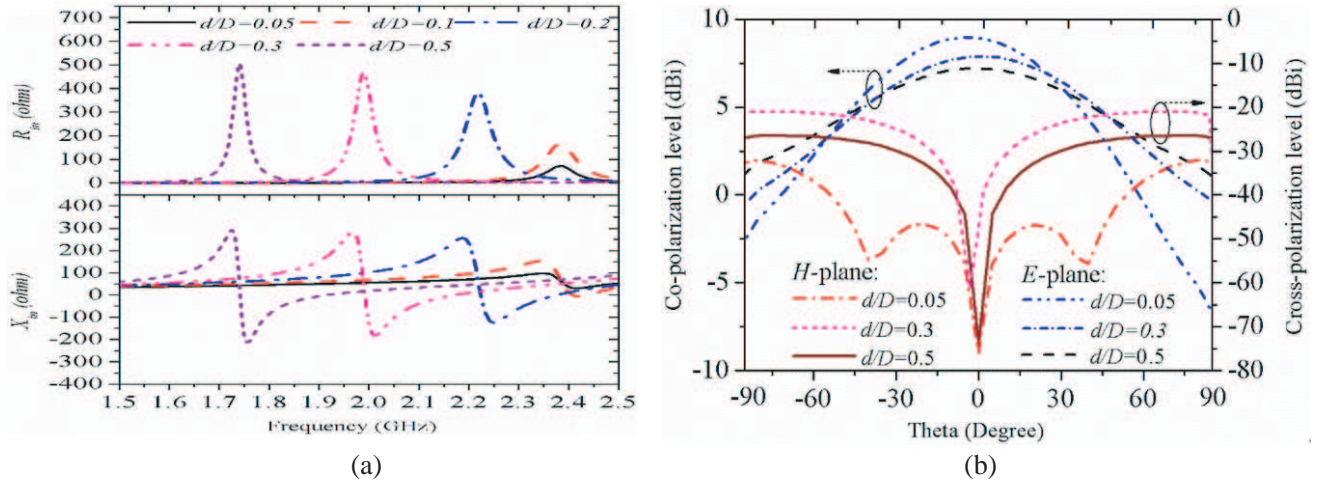


Figure 5. (a) Simulated input resistance and reactance, and (b) simulated co-polarization in E -plane and cross-polarization in H -plane of the pair of shorting posts loaded CMSA with different d/D ratio. (At $d/D = 0.5, 0.3$ and 0.05 the corresponding modified frequencies are $F_F = 1.74, 2.214$ and 2.45 GHz, respectively).

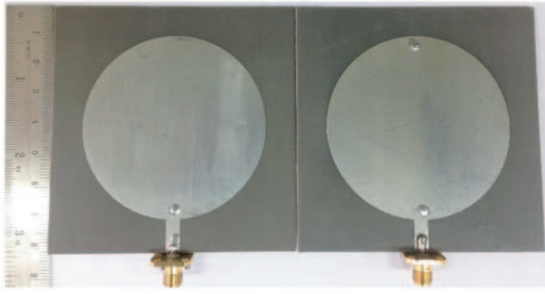
of CMSA with a pair of shorting posts for three different cases of position of the pair of shorting posts at corresponding frequency F_F . It is noted that current distribution is nearly symmetrical along the centerline XX' and also on a patch for all shorting positions, resulting in reduced cross-polarization levels.

Figure 5(a) shows the simulated input resistance (R_{in}) and reactance (X_{in}) for different d/D ratios of the pair of shorting posts loaded CMSA. It is observed that as d/D ratio decreases, i.e., $d/D = 0.5$ to 0.05 , the input impedance at F_F gets reduced from 504 to 50Ω while the corresponding resonant frequency F_F is increased from 1.740 to 2.450 GHz. The increase in the resonant frequency F_F of the shorted CMSA is due to the modified symmetrical current distribution caused by a pair of shorting posts. The proper matching for a pair of shorting posts loaded CMSA with 50Ω -MS-line feed is obtained at F_F for $d/D = 0.05$. Fig. 5(b) depicts the co-polarization in E -plane and cross-polarization in H -plane for three cases of d/D of a pair of shorting posts loaded CMSA. There is a substantial reduction of cross-polar level in the H -plane compared to that of a single shorting post CMSA as shown in Fig. 3(b). The improvement is more than 24 dB for $d/D = 0.05$. For $d/D = 0.5$ both the configurations become a center shorted CMSA with identical response. The E -plane co-polarization levels are similar for all the positions of shorting posts. Two identical pairs of shorting posts are symmetrically loaded in the proposed configuration, which results in the decrement of H -plane cross-polar level as compared to the single shorted 50Ω -MS-line fed CMSA. This decrease in the cross-polarization level results in 1 dB improvement in the value of directivity for $d/D = 0.05$ in comparisons with the corresponding case of single shorted CMSA.

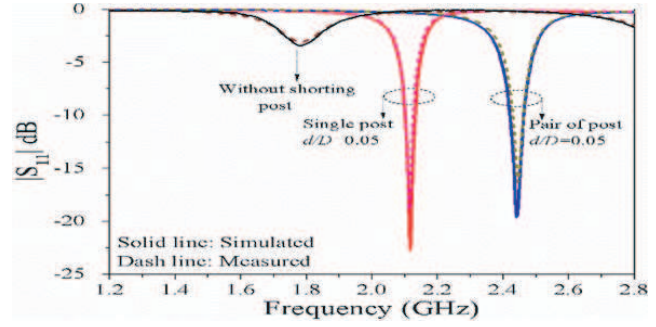
5. EXPERIMENTAL VALIDATIONS AND DISCUSSIONS

For verification of the proposed configuration, two antennas with single shorting post and a pair of shorting posts are fabricated on an Arlon dielectric substrate with $\epsilon_r = 2.5$, $h = 1.59$ mm and $\tan \delta = 0.003$. The shorting post with radius 0.5 mm is located at $d/D = 0.05$, for both the configurations. CMSAs are fed with 50Ω -MS-line of $W_s = 4.538$ mm and length of 10 mm. Ground plane dimension is 80×80 mm², for both the antenna configurations. Actual photographs of CMSAs are shown in Fig. 6(a). Measurements have been carried out in reflection free environment with the help of Agilent-Fieldfox-Vector Network Analyzer and standard dual ridge horn antenna for transmission, which is placed in far-field distance of the antenna under test. Simulated and measured results are compared in Figs. 6–8, which are in good agreement.

Figure 6(b) compares simulated and measured return losses for fundamental and modified fundamental modes frequencies (at F_F) for the 50Ω -MS-line feed CMSA without shorting post, with



(a)



(b)

Figure 6. (a) Photographs of proposed single shorting post and a pair of shorting posts loaded CMSA with shorting posts at $d/D = 0.05$, and (b) comparison of simulated and measured return losses for without shorting post, with single shorting post and a pair of shorting posts loaded CMSAs.

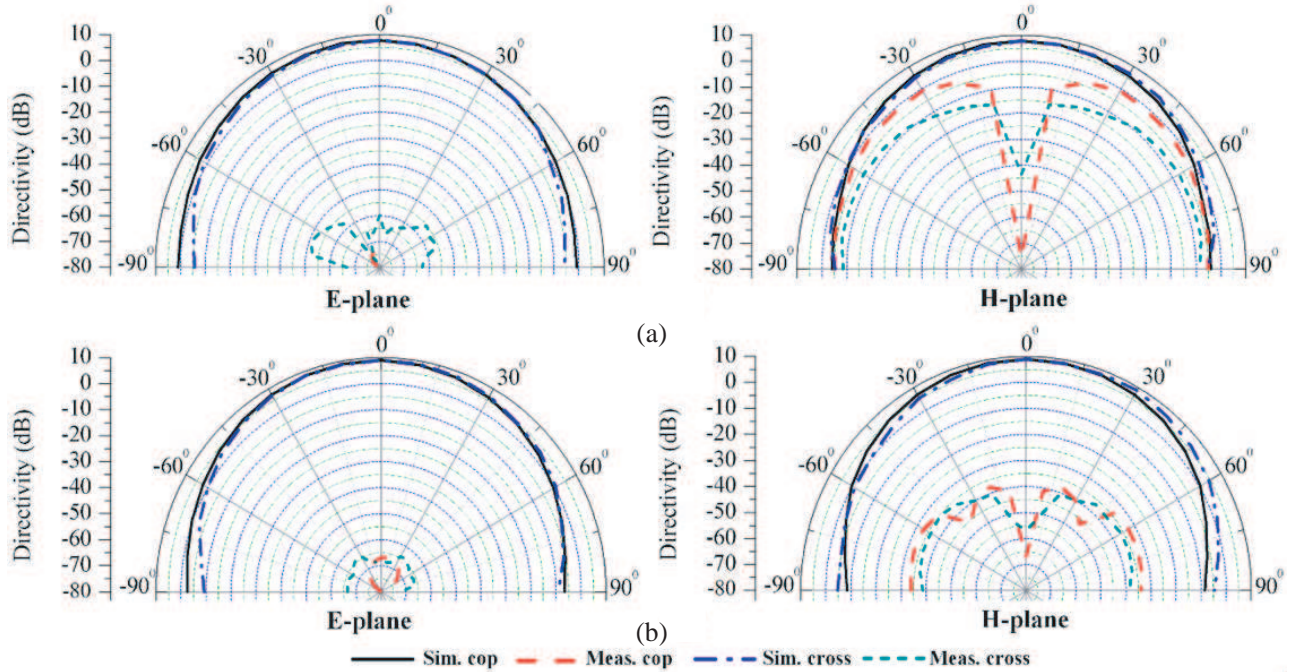


Figure 7. Comparison of simulated and measured radiation patterns in E -plane and H -plane; (a) single shorted CMSA at 2.095 GHz and (b) a pair of shorting posts loaded CMSA at 2.45 GHz.

single shorting post, and a pair of shorting posts, respectively. The CMSA with $50\ \Omega$ -MS-line feed without shorting post has high resonant input resistance, thus it does not match with the MS-line feed. The simulated and measured resonant frequencies for the same case are 1.742 GHz and 1.751 GHz, respectively. With single shorting post and a pair of shorting posts, the input impedance is close to $50\ \Omega$, leading to a good input impedance matching with the MS-line feed. For a single shorting post CMSA, the simulated and measured modified F_F are 2.095 GHz and 2.093 GHz, respectively with % bandwidth (BW) of 1.6 and 1.54. Similarly, for the CMSA with a pair of shoring posts, the simulated modified F_F is 2.450 GHz against the measured value of 2.453 GHz, with % BW of 2.02 and 1.90, respectively. Fig. 7 shows comparisons of simulated and measured radiation patterns in E -plane and H -plane for proposed configurations. The maximum radiation is in the broadside direction for both proposed configurations. In Fig. 7(a), for E -plane of a single shorting post CMSA, the simulated cross-polarization levels are less than -60 dB, whereas the corresponding measured level is less than -70 dB. Similarly, in H -plane the cross-polar levels are very high because of the asymmetrical current distribution. The maximum simulated level is -5 dB, whereas the measured level is -10 dB.

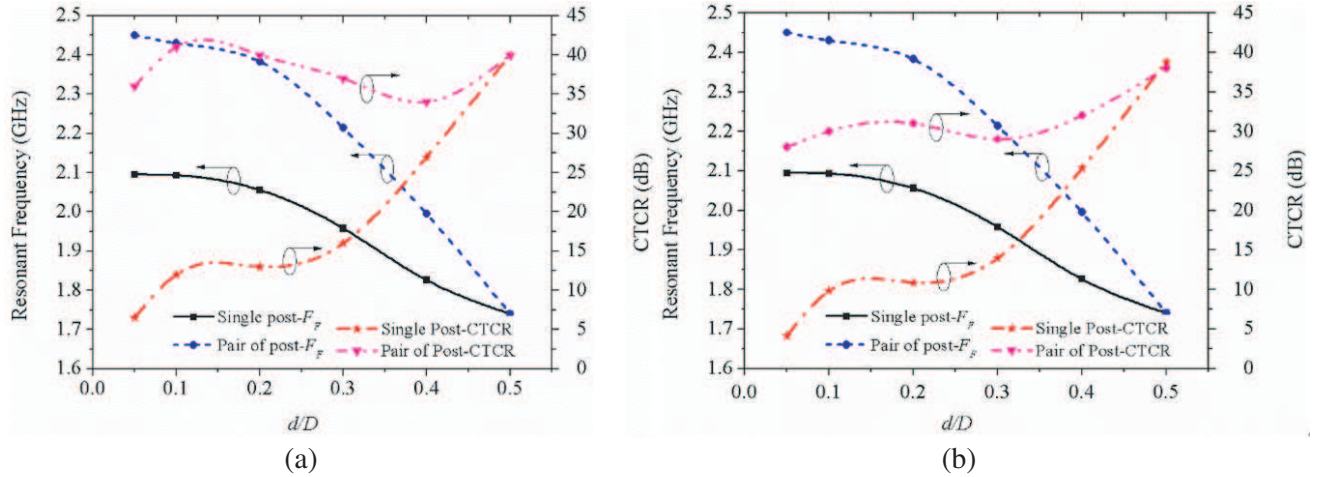


Figure 8. Comparison of simulated CTCR values of a single shorting post and a pair of shorting posts CMSAs for (a) $\theta = \pm 30^\circ$, and (b) $\theta = \pm 60^\circ$ with different d/D ratio at corresponding modified F_F .

In Fig. 5(b), for the case of E -plane of a pair of shorting posts CMSA, the simulated cross-polar levels are less than -65 dB, whereas the measured level is less than -60 dB. However, in H -plane of a pair of shorting post CMSA, the cross-polarization levels with symmetric current distribution are much suppressed. The maximum simulated level is -40 dB, whereas the measured level is -45 dB. This is marked improvement as compared to single shorting post CMSA and even to the reported RMSA with a pair of shorting posts [15]. Fig. 8 shows the comparison of CTCR values of single shorting post and a pair of shorting posts CMSAs for angles $\theta = \pm 30^\circ$ and $\pm 60^\circ$, with different d/D ratios at corresponding modified F_F . Table 1 gives the comparison of CTCR values of a single shorting post and a pair of shorting posts CMSAs in H -plane, within an angular range of $-30^\circ \leq \theta \leq 30^\circ$ and $-60^\circ \leq \theta \leq 60^\circ$. The CTCR values of a pair of shorting posts CMSA are at least 24 dB, which is far better than that of a single shorting post CMSA for both the angular ranges in H -plane as notice from Fig. 8 and Table 1. This is again a notable improvement of the value of CTCR as compared to that obtained from an RMSA reported in [14–16]. The total volume of the proposed antenna structure is $0.0022\lambda_0^3$ including ground plane. It has also been seen that the sensitivity of resonance frequency with respect to the position of the shorting post of 50Ω -MS-line-fed CMSA is more prominent than RMSA [16]. The proposed feeding method can be etched on a same substrate to provide a better planner structure, which is desirable for an on-chip platform in direct integration.

Table 1. Comparisons of cross-polarization ratios.

Sr. No	Configurations CMSA	Cross-Polarization ratio (dB)			
		$\theta \in (-30^\circ, 30^\circ)$		$\theta \in (-60^\circ, 60^\circ)$	
		Sim.	Meas.	Sim.	Meas.
1	Paired of shorting posts ($d/D = 0.05$)	36	45	28	37
2	Single shorting post ($d/D = 0.05$)	6.5	17	1.8	13

6. CONCLUSIONS

In this paper, shorting posts have been used to reduce the input impedance on the periphery of the CMSA, which enables direct matching with 50Ω -MS-line feed. The peripheral impedance of the CMSA is adjusted to a wide range by selecting a proper position of the shorting posts. The CTCR values of

the pair of shorting posts CMSA have more than 24 dB improvement with that of a single shorting post CMSA. Also, $50\ \Omega$ -MS-line feed eliminates the use of separate TRL calibration kit, for de-embedding the real input impedance. Simulation results are validated through measurements with good agreement. The proposed work provides an insight into the functioning of widely used CMSA element with shorting posts, which will be helpful in designing series and corporate feeds for antenna arrays.

ACKNOWLEDGMENT

The authors would like to thank S. S. Kakatkar and Jagdish Prajapatee from RFMS Division, SAMEER, Mumbai for their kind help in fabrication and valuable input during experimental measurement. The authors would also like to thank TEQIP-III of VJTI-Mumbai for their financial support.

REFERENCES

1. Waterhouse, R., "Small microstrip patch antenna," *Electronics Letters*, Vol. 31, No. 8, 604–605, 1995.
2. Kumar, G. and K. P. Ray, *Broadband Microstrip Antennas*, Artech House, Norwood, MA, USA, 2003.
3. Wong, K. L., *Compact and Broadband Microstrip Antennas*, John Wiley & Sons, Inc., New York, 2002.
4. Satpathy, S. K., K. P. Ray, and G. Kumar, "Compact shorted variations of circular microstrip antennas," *Electronics Letters*, Vol. 34, No. 2, 137–138, 1998.
5. Wong, K. L. and W. S. Chen, "Compact microstrip antenna with dual-frequency operation," *Electronics Letters*, Vol. 33, No. 8, 646–647, 1997.
6. Deshmukh, A. A. and K. P. Ray, "Broadband shorted sectoral microstrip antenna," *Progress In Electromagnetics Research C*, Vol. 20, 55–65, 2011.
7. Podilchak, S. K., A. P. Murdoch, and Y. M. M. Antar, "Compact, microstrip-based folded-shortened patches: PCB antennas for use on microsattelites," *IEEE Antennas Propag. Mag.*, Vol. 59, No. 2, 88–95, April 2017.
8. Rezaazadeh, N. and L. Shafai, "A compact microstrip patch antenna for civilian GPS interference mitigation," *IEEE Antennas Wireless Propag. Lett.*, Vol. 17, No. 3, 381–384, March 2018.
9. Chakravarty, T. and A. De, "Design of tunable modes and dual-band circular patch antenna using shorting post," *IEE Proc. — Microw., Antennas Propag.*, Vol. 146, No. 3, 224–228, 1999.
10. Porath, R., "Theory of miniaturized shorting-post microstrip antennas," *IEEE Trans. Antennas Propag.*, Vol. 48, No. 1, 41–47, Jan. 2000.
11. Row, J. S., "A simple impedance-matching technique for patch antennas fed by coplanar microstrip line," *IEEE Trans. Antennas Propag.*, Vol. 53, No. 10, 3389–3391, Oct. 2005.
12. Schaubert, D., F. Farrar, A. Sindoris, and S. Hayes, "Microstrip antennas with frequency agility and polarization diversity," *IEEE Trans. Antennas Propag.*, Vol. 29, No. 1, 118–123, Jan. 1981.
13. Chapari, A., A. Zeidaabadi Nezhad, and Z. H. Firouzeh, "Analytical approach for compact shorting pin circular patch antenna," *IET Microwaves Antennas Propag.*, Vol. 11, No. 11, 1603–1608, 2017.
14. Zhang, X. and L. Zhu, "An impedance-agile microstrip patch antenna with loading of a shorting pin," *2015 Asia-Pacific Microwave Conference (APMC)*, 1–3, 2015.
15. Zhang, X. and L. Zhu, "Patch antennas with loading of a pair of shorting pins toward flexible impedance matching and low cross polarization," *IEEE Trans. Antennas Propag.*, Vol. 64, No. 4, 1226–1233, April 2016.
16. Rathod, S. M., R. N. Awale, and K. P. Ray, "Analysis of a single shorted rectangular microstrip antenna for $50\ \Omega$ microstrip line feed," *2016 International Symposium on Antennas and Propagation (APSYM)*, 1–4, Cochin, 2016.